Screened Hydrogenic Model

D. T. Bishel[1, 2, a)]
[1)]*Department of Physics and Astronomy, University of Rochester*
[2)]*Laboratory for Laser Energetics, University of Rochester*

(Dated: 26 October 2023)

This document describes the implementation of the screened hydrogenic model and its applications.

I. MODEL

The screened hydrogenic model is a computationally inexpensive atomic model for estimating material and radiative properties of any ionization state of any element.[1] Correlations between bound electrons are treated through a screening matrix. The screening matrix describes how the i^{th} electron reduces the effective nuclear charge acting on the j^{th} electron. Hydrogenic equations modified by the screening are employed to calculate level energies, oscillator strengths, excitation rates, and other atomic data. The model is approximate yet computationally inexpensive. Due to its simplicity, the model can be modified and applied to a range of problems. We discuss a few of the variations and applications in the following section.

This implementation primarily follows the concise presentation in Chapter 10 of Atzeni and Meyer-ter Vehn's *The Physics of Inertial Fusion*[?] . An early and insightful description of the different flavors of the screened hydrogenic model can be found in Harris Mayer's 1947 Los Alamos Scientific Laboratory Report[1]. Additional terms, notably the pressure-induced occupation factor, are from the more recent article by Zimmerman and More[2].

A. Isolated Atom with Prescribed Occupations

The simplest implementation considers a single atom with prescribed shell occupations $\vec{P} = \{P_n\}$ and nuclear charge Z. The defining characteristic of this model is that there is no reference to any plasma thermodynamic state or properties. Namely, the considered atom is entirely isolated from any perturbing environment. All terms originate from bound electrons belonging to the ion, hence prescription of the shell occupations.

A straightforward description is found in Atzeni and Meyer-ter-Vehn.[3] The effective nuclear charges Q_n seen by the n^{th} shell due to screening by inner- and same-shell electrons is

$$Q_n = Z - \sum_{m \leq n} \sigma_{nm} P_m. \tag{1}$$

σ_{nm} are the elements of the screening matrix.[1] The screening W_n of the n^{th} shell by the outer electrons is

$$W_n = \sum_{m \geq n} \frac{P_m Q_m}{m^2} \sigma_{mn}. \tag{2}$$

Note that the order of the indexing of σ is reversed in this equation. The energy E_n of the n^{th} shell is that of the hydrogenic atom, with effective nuclear charge Q_n and additional screening W_n by outer electrons:

$$E_n = E_A \left(W_n - \frac{Q_n^2}{2n^2} \right) \tag{3}$$

where $E_A = 27.2$ eV. The ground state energy of the configuration is

$$E^{tot}_{i,s=0} = E_A \sum_m \left(- \frac{Q_m^2}{2m^2} P_m \right) \tag{4}$$

This fully defines the structure of the atom, and E_n, P_n, and E^{tot} can be used to derive further properties. See Fig. 1 for the workflow.

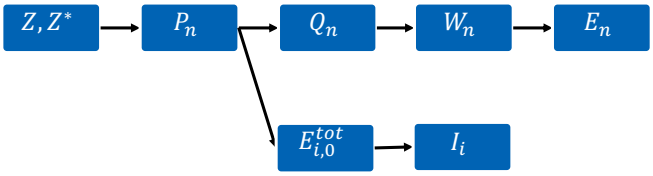

FIG. 1. Workflow for an isolated atom with prescribed shell populations. Black arrows indicate dependencies. See Sec. I A for description of quantities and equations.

As an example, this can be used to calculate the ionization potentials of a given element. An ensemble of Z screened hydrogenic atoms with nuclear charge Z is constructed in which each atom corresponds to the ground state of a different ionization state $\bar{Z}$ of the atom. For a given $\bar{Z}$, the $Z - \bar{Z}$ electrons are assigned to the lowest available shell without exceeding the maximum shell occupation of $2n^2$. For lithium, this requires the set of $\vec{P}$ $[2,1,0,...]$, $[2,0,0,...]$, and $[1,0,0,...]$ corresponding to the ground states of the neutral atom, singly-ionized ion, and doubly-ionized ion, respectively. The ionization potential is then calculated by taking the difference in ground-state energies $E^{tot}_{i,0}$ between neighboring ions i and $i+1$.

B. Average Ion Model

A real plasma consists of many ions occupying a variety of quantum states in thermodynamic equilibrium with each

[a)]Electronic mail: dbishel@ur.rochester.edu

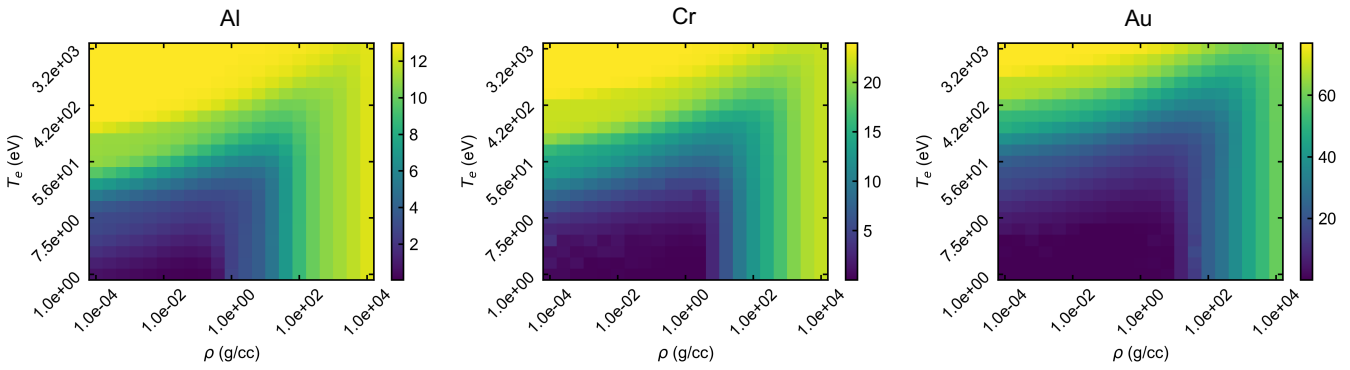

FIG. 2. Mean ionization state $\bar{Z}$ of Al, Cr, and Au as a function of temperature and mass density. Calculated using the procedure outlined in Sec. I B.

other and the free electron population. To incorporate the distribution of quantum states and the influence of the circumfluent plasma, the screened hydrogenic model infrastructure can be deployed within an average-ion framework. Instead of representing just one of many possible states, the screened-hydrogenic average-ion conceives a fictitious ion of fractional charge and fractional shell populations, representing the average quantum state of all ions. Plasma effects are introduced by allowing P_n to fluctuate in response to a prescribed temperature T and density ρ. Dense plasma effects can be included through thermodynamic terms such as chemical potential and continuum lowering.

1. Algorithm

To initiate the model, mass density ρ, temperature T, and a trial mean ionization state $\bar{Z}$ are given. These are used to calculate the chemical potential μ of the plasma, the ionization potential depression ΔE_c (IPD), and a pressure-induced occupation factor g_n. Next, g_n is solved self-consistently with Fermi-distributed shell populations P_n, the screened nuclear charges Q_n, and orbit radii R_n. The energy levels E_n are determined self-consistently with P_n, Q_n, and W_n. The mean ionization state $\bar{Z}$ can then be calculated by summing over the P_n of bound levels, defined as those having $E_n + \Delta E_c > 0$. This entire loop must be iterated to achieve convergence between the input $\bar{Z}$ and the calculated $\bar{Z}$. Definitions and equations are shown in Table I, and a graph of the workflow is shown in Fig. 3.

A consequence of coupling the atom to the plasma environment is that $\bar{Z}$ has no closed form solution. A self-consistent solution must be found by iterating over circularly dependent equations until the calculated value equals the input value to within some tolerance. There are three such loops: (1) $g_n - P_n - Q_n - R_n$, (2) $P_n - Q_n - W_n - E_n$, and (3) the entire calculation of $\bar{Z}$. If the difference in calculated and input values exceeds the user-specified tolerance, the new input value is taken as a linear mixing of the previous input value and the

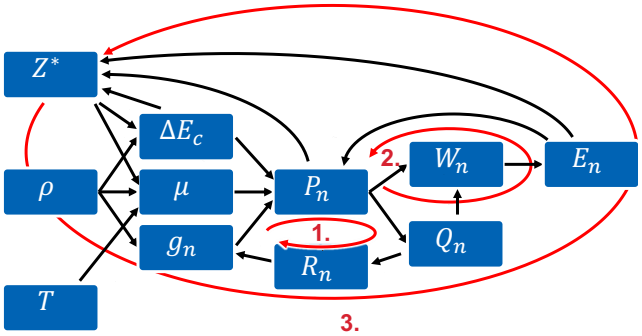

FIG. 3. Average ion workflow. Black arrows indicate dependencies. Red arrows indicate recursive loops requiring a self-consistent solution. The red arrow begins and ends on the quantity requiring iteration. The order in which the self-consistent loops should be performed is noted by the red numbers. See Sec. I B for description of quantities and Table I for equations.

calculated value:

$$f_{input}^{new} = (1-c) \times f_{input}^{old} + c \times f_{calc}^{old}. \quad (5)$$

Values of the mixing coefficient $c \in (0,1)$ are chosen to aid convergence. Values near 0.5 tend to be optimal.

Further quantities can be derived from the converged solution. For instance, one can use E_n as the set of average energy levels, and R_n as the set of average shell radii.

Through inclusion of μ, ΔE_c[4,5], and g_n, this model approximates the impact of the dense plasma environment on P_n and $\bar{Z}$. Various IPD models can be implemented.

2. Results

$\bar{Z}$ of Al, Cr, and Au are plotted in Fig. 2, all using the same code described above. Each element displays typical ionization behavior. For a given density, increasing temperature re-

TABLE I. Quantities and equations used in the average ion model.

Quantity	Symbol	Equation
Ionization potential depression (IPD)	ΔE_c	$\frac{3}{2}\frac{\bar{Z}e^2}{R_0}$
Chemical potential	μ	$k_BT\left[-\frac{3}{2}\ln\Theta+\ln\frac{4}{3\sqrt{\pi}}+\frac{A\Theta^{-(b+1)}+B\Theta^{-(b+1)/2}}{1+A\Theta^{-b}}\right]$ $A=0.250254,\quad B=0.072,\quad b=0.858$
Degeneracy parameter	Θ	T/T_F
Pressure-induced occupation factor	g_n	$\frac{2n^2}{1+\left(a\frac{R_n}{R_0}\right)^b}$
Shell radius	R_n	$a_0\frac{n^2}{Q_n}$
Ion-sphere radius	R_0	$\left(\frac{3Am_p}{4\pi\rho}\right)^{1/3}$
Fermi-distributed shell populations	P_n	$\frac{g_n}{1+\exp\left[\frac{E_n+\Delta E_c-\mu}{k_BT}\right]}$
Mean ionization state	$\bar{Z}$	$Z-\sum_n P_n$, bound states n having $E_n+\Delta E_c>0$

sults in increasing ionization. At a given temperature, increasing density initially leads to lower ionization as predicted by the Saha ionization balance, which is valid for low densities. At sufficiently high density, free electrons in the circumfluent plasma screen the bound electrons from the nucleus, reducing their ionization potential. This process is referred to as pressure ionization.

C. Multiconfiguration Model

When predicting state-specific information such as spectroscopic line positions, models which combine all states into a single average ion are insufficient. One must instead track the population or number of ions that occupy each quantum state. This can be implemented by considering an ensemble of screened hydrogenic atoms with prescribed populations corresponding to the many possible excited states of the possible ionization states of the element. That is, one must not only include $\vec{P}=[2,0,0,...]$ for the ground state of a helium-like ion, but also $[1,1,0,...]$, $[1,0,1,...]$, $[0,2,0,...]$ and so on. Thermodynamic equilibrium dictates the state populations. In general, all states which hold appreciable population should be included in the multiconfiguration model, as should states that participate in radiative transitions of interest. The isolated atom model of Sec. I A is then run on each prescribed state individually to obtain that state's atomic structure, most notably E_n.

1. Populations

With the atomic structure in hand for all states, the population of each state is calculated. Under the assumption of local thermodynamic equilibrium, the ratio of number densities of neighboring ionization states j and $j-1$ is given by the Saha equation modified for electrostatic interactions with the plasma medium[4]

$$\frac{N_j}{N_{j-1}}=\frac{2}{N_e\lambda_{th}^3}\frac{G_j}{G_{j-1}}\exp\left(-\frac{I_j-\Delta E_c}{kT}\right), \tag{6}$$

where $\lambda_{th}=\left(2\pi\hbar^2/m_ekT\right)^{1/2}$ is the electron thermal wavelength and $G_j=\sum_s g_s\exp\left[-(E_{j,s}-E_{j,0})/kT\right]$ is the internal partition function for excited state s with statistical weight g_s and energy $E_{j,s}$. The ratio of any two excited states s and s' belonging to the same ionization state j is found from the Boltzmann factor[6]

$$\frac{n_{j,s}}{n_{j,s'}}=\exp\left(-\frac{E_{j,s}-E_{j,s'}}{kT}\right). \tag{7}$$

To obtain the joint solution of Eqs. 6 and 7 and the resulting Saha-Boltzmann balance, consider a plasma at electron density N_e and temperature T consisting of N_{tot} ions of nuclear charge Z. The ions are allowed to occupy any ionization state j, from the neutral atom ($j=0$) to the bare ion ($j=Z$). The ionization potentials I_j and energy levels $E_{j,s}$ of each ionization state j and excited state s are calculated from the isolated atom model of Sec. I A. The population ratio c_j of ionization state j relative to the neutral atom is given by a cumulative product over Eq. 6:

$$\begin{aligned} c_j &= \prod_{j'=1}^{j}\frac{N_{j'}}{N_{j'-1}} \\ &= \frac{N_1}{N_0}\times\frac{N_2}{N_1}\times\frac{N_3}{N_2}\times\cdots\times\frac{N_j}{N_{j-1}} \\ &= \frac{N_j}{N_0}, \end{aligned} \tag{8}$$

where the ratios $N'_j/N_{j'-1}$ are constructed from Eq. 6. By

conservation of particles, the total ion density is

$$\begin{aligned} N_{\rm tot} &= \sum_{j=0}^{Z} N_j \\ &= N_0(1+\sum_{j=1}^{Z} c_j) \end{aligned} \tag{9}$$

Rearranging this equation, we can define the fractional abundance $p_0^{\rm Saha}$ of the neutral atom:

$$p_0^{\rm Saha} \equiv \frac{N_0}{N_{\rm tot}} = \left[1+\sum_{j=1}^{Z} c_j\right]^{-1} \tag{10}$$

The fractional abundance $p_j^{\rm Saha}$ of all other ionization states j can then be written as

$$\begin{aligned} p_j^{\rm Saha} &\equiv \frac{N_j}{N_{\rm tot}} \\ &= \left[\frac{N_j}{N_{j-1}} \times \frac{N_{j-1}}{N_{j-2}} \times \cdots \times \frac{N_2}{N_1} \times \frac{N_1}{N_0}\right] \times \frac{N_0}{N_{\rm tot}} \\ &= c_j \times p_0^{\rm Saha}. \end{aligned} \tag{11}$$

Useful for casting the multiconfiguration model in terms of ion or mass density, with all $p_j^{\rm Saha}$ known, the mean ionization state $\bar{Z}$ and total ion density $N_{\rm tot}$ can be calculated as

$$\bar{Z} = \sum_{j=0}^{Z} j \times p_j^{\rm Saha} \tag{12}$$

$$N_{\rm tot} = N_{\rm e}/\bar{Z} \tag{13}$$

The Boltzmann factor is invoked to distribute the density N_j within an ionization state to each of the constituent excited states s. From Eq. 7, the density ratio between excited state s and the ground state is $\frac{N_{j,s}}{N_{j,0}} = \exp[-(E_{j,s}-E_{j,0})/kT]$. By conservation of particles, an ion with possible states consisting of the ground state ($s=0$) and $\mathscr{N}$ excited states (s indexed 1 through $\mathscr{N}$) will obey

$$\begin{aligned} N_j &= \sum_{s=0}^{\mathscr{N}} N_{j,s} \\ \Rightarrow \frac{N_j}{N_{j,0}} &= 1+\sum_{s=1}^{\mathscr{N}} \frac{N_{j,s}}{N_{j,0}} \\ &= 1+\sum_{s=1}^{\mathscr{N}} \exp\left(-\frac{E_{j,s}-E_{j,0}}{kT}\right) \end{aligned} \tag{14}$$

Rearranging, we can obtain the following equation for the ground state population

$$N_{j,0} = N_j \times \left[1+\sum_{s=1}^{\mathscr{N}} \exp\left(-\frac{E_{j,s}-E_{j,0}}{kT}\right)\right]^{-1} \tag{15}$$

Now, $N_{j,s} = N_{j,0} \times \exp\big[-(E_{j,s}-E_{j,0})/kT\big]$ from Eq. 7, which, upon substitution of Eq. 15 and division by N_j, becomes

$$p_{j,s}^{\rm Boltz} \equiv \frac{N_{j,s}}{N_j} = \frac{\exp\big[-(E_{j,s}-E_{j,0})/kT\big]}{1+\sum_{s'=1}^{\mathscr{N}} \exp\big[-(E_{j,s'}-E_{j,0})/kT\big]}. \tag{16}$$

Combining Eqs. 11 and 16, the number density $N_{j,s}$ of excited state s of ionization state j is

$$N_{j,s} = p_j^{\rm Saha} \times p_{j,s}^{\rm Boltz} \times N_{\rm tot} \tag{17}$$

[1] H. Mayer (Los Alamos, NM, 1949) pp. 1–151.
[2] G. B. Zimmerman and R. M. More, J. Quant. Spectrosc. Radiat. Transf. **23**, 517 (1980).
[3] S. Atzeni and J. Meyer-ter Vehn, *The Physics of Inertial Fusion : Beam Plasma Interaction, Hydrodynamics, Hot Dense Matter*, 1st ed., International Series of Monographs on Physics, vol. 125 (Oxford University Press, Oxford, United Kingdom, 2004).
[4] G. Ecker and W. Kröll, Phys. Fluids **6**, 62 (1963).
[5] J. C. Stewart and K. D. Pyatt, Astrophys. J. **144**, 1203 (1966).
[6] R. D. Cowan, *The Theory of Atomic Structure and Spectra*, Los Alamos series in basic and applied sciences (University of California Press, Berkeley, 1981).
[7] S. B. Hansen, E. C. Harding, P. F. Knapp, M. R. Gomez, T. Nagayama, and J. E. Bailey, High Energy Density Phys. **24**, 39 (2017).